

Localized Basis Method in OpenMX

1. Introduction

2. Implementation

- ✓ Basis functions
- ✓ Numerical grid
- ✓ Pseudopotentials

3. Ongoing developments

4. Summary

Short history of OpenMX

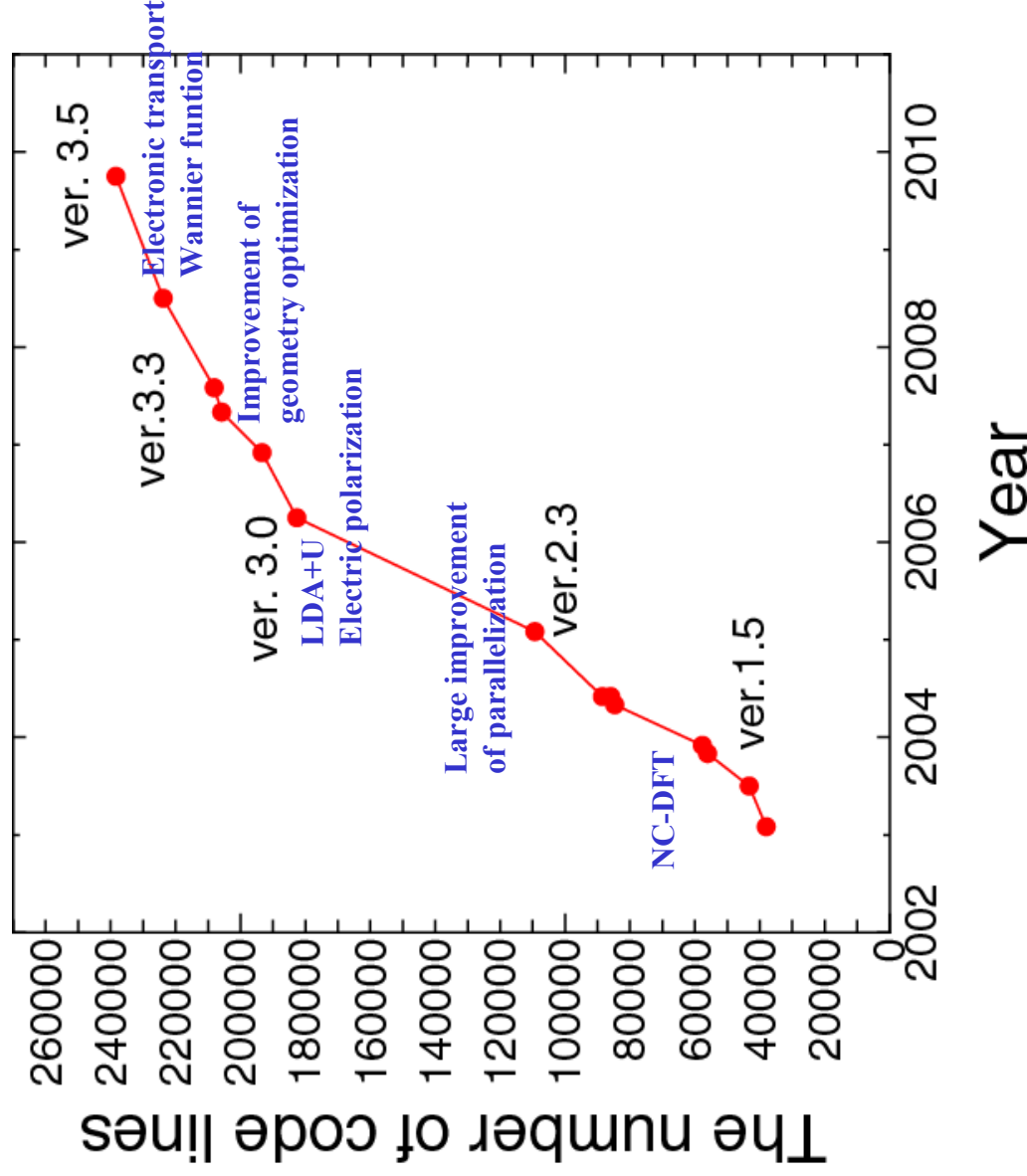
The development of the code has been **started** from the middle of **2000**.

The first public release was done at January 2003, and **fifteen releases** were made **until now**.

The code has been steadily developed as shown in the figure, and the community itself has been also growing.

About 80 related papers have been published.

The number of lines of the code



Contributors

- T. Ozaki (JAIST)
- H. Kino (NIMS)
- J. Yu (SNU)
- M. J. Han (Columbia Univ.)
- N. Kobayashi (Tsukuba Univ.)
- M. Ohfuti (Fujitsu)
- F. Ishii (Kanazawa Univ.)
- T. Ohwaki (Nissan)
- H. Weng (JAIST)
- M. Toyoda (JAIST)
- K. Terakura (JAIST)

OpenMX **Open** source package for **Material eXplorer**

Basic methods:

Functional:	LDA, GGA, LDA+U
Basis function:	Localized pseudoatomic basis functions
Treatment of core:	Norm-conserving pseudopotentials (PP)
Poisson solver:	Fast Fourier transform (FFT)
Integration method:	Regular mesh + projector expansion method
Eigenvalue solver:	Householder+QR methods
Geometry opt.:	BFGS and eigenvector following (EF) methods
Parallelization:	MPI+OpenMP

Extensions:

O(N) eigenvalue solver:	Krylov subspace, divide-conquer methods
Non-collinear DFT:	Two-component spinor with constrained schemes
Relativistic effects:	Fully relativistic PP with spin-orbit coupling
Electronic polarization:	Berry phase scheme
Electronic transport:	Ballistic transport by NEGF
Wannier function (WF):	Maximally localized WF and mapping to a TB model
.....	

Kohn-Sham (KS) equation

3D coupled non-linear differential equations have to be solved self-consistently.

$$\hat{H}_{\text{KS}}\phi_i = \varepsilon_i\phi_i \quad \hat{H}_{\text{KS}} = -\frac{1}{2}\nabla^2 + v_{\text{eff}}$$

$$\rho(\mathbf{r}) = \sum_i^{\text{occ}} \phi_i^*(\mathbf{r})\phi_i(\mathbf{r})$$

$$\nabla^2 v_{\text{Hartree}}(\mathbf{r}) = -4\pi\rho(\mathbf{r})$$

$$v_{\text{eff}} = v_{\text{ext}}(\mathbf{r}) + v_{\text{Hartree}}(\mathbf{r}) + \frac{\delta E_{\text{xc}}}{\delta\rho(\mathbf{r})}$$

Input charge = Output charge \rightarrow Self-consistent condition

Classification of the KS solvers

Treatment of core electrons

All electron (AE) method

Pseudopotential (PP) method

Plane wave basis (PW)

Mixed basis (MB)

Localized systematic basis (LSB)

Localized atomic basis (LB)

Basis functions

AE+MB: FLAPW

AE+LB: Gaussian

PP+PW: Plane wave with PP

PP+LSB: FEM, FDM, wavelet

PP+LB: OpenMX, SIESTA

Accuracy Efficiency

◎ ×

○ ○

○ ○

○ ○

△ ◎

LCPAO method

(Linear-Combination of Pseudo Atomic Orbital Method)

One-particle KS orbital

$$\psi_{\sigma\mu}^{(\mathbf{k})}(\mathbf{r}) = \frac{1}{\sqrt{N}} \sum_{\mathbf{n}} e^{i\mathbf{R}_{\mathbf{n}} \cdot \mathbf{k}} \sum_{i\alpha} c_{\sigma\mu, i\alpha}^{(\mathbf{k})} \phi_{i\alpha}(\mathbf{r} - \mathbf{T}_i - \mathbf{R}_{\mathbf{n}}),$$

is expressed by a linear combination of atomic like orbitals in the method.

$$\phi(\mathbf{r}) = Y_l^m(\hat{\mathbf{r}})R(r)$$

Features:

- It is easy to interpret physical and chemical meanings, since the KS orbitals are expressed by the atomic like basis functions.
- It gives rapid convergent results with respect to basis functions due to physical origin. (however, it is not a complete basis set, leading to difficulty in getting full convergence.)
- The memory and computational effort for calculation of matrix elements are $O(N)$.
- It well matches the idea of linear scaling methods.

Why we employ “PP+LB” scheme?

Many of systems we are interested in include more than 100 atoms. Usually, a lot of systematic calculations for such systems have to be performed in order to comprehensively understand the physics and chemistry of the systems.

Thus, the situation in the actual applications of DFT evidently requires the development of a fast solver of the KS method.

We consider that the “PP+LB” scheme can provide a fast solver for the requirement in a balanced way with respect to accuracy and efficiency.

How about accuracy?

If we are careful enough so that we can spend some time to tune basis functions and pseudopotentials and validate their quality, then the “PP+LB” method can reproduce results by the AE methods and the “PP+PW” methods with considerable accuracy.

However, the convergence of the localized basis functions is not so systematic like PW. This is a well-known problem and can be disadvantage in “PP+LB”.

The tuning process is troublesome in general especially for beginners. But we think that the tuning process itself is a way to understand specific features of each element and chemical environment in molecules and bulks.

Accuracy: Ground state of molecules

Ground state calculations of dimers

PRB 69, 195113 (2004)

Dimer	Expt.	Calc.	Dimer	Expt.	Calc.
H ₂ (H4.5-s2)	1Σ ⁺ _g ⁺ a	1Σ ⁺ _g ⁺ (1s _g ²)	K ₂ (K10.0-s2p2)	1Σ ⁺ _g ⁺ f	1Σ ⁺ _g ⁺ (3pπ _g ⁴ 3pσ _u ² 4sσ _g ²)
He ₂ (He7.0-s2)	1Σ ⁺ _g ⁺ b	1Σ ⁺ _g ⁺ (1s _g ² 1s _u ²)	CaO (Ca7.0-s2p2d2)	1Σ ⁺ _g ⁺ k	1Σ ⁺ _g ⁺ (sσ _g ² sσ _u ² pπ _u ⁴)
Li ₂ (Li8.0-s2)	1Σ ⁺ _g ⁺ c	1Σ ⁺ _g ⁺ (2s _g ²)	ScO (Sc7.0-s2p2d2)	2Σ ⁺ _g ⁺ l	2Σ ⁺ _g ⁺ (dπ ⁴ sσ ² sσ ¹)
BeO (Be6.0-s2p2)	1Σ ⁺ _g ⁺ d	1Σ ⁺ _g ⁺ (sσ ² sσ ² pπ ⁴)	Ti ₂ (Ti7.0-s2p2d2)	3Δ _g ⁺ m	3Δ _g ⁺ (4sσ _g ² 3dσ _g ¹ 3dπ _u ⁴ 3dδ ¹)
B ₂ (B5.5-s2p2)	3Σ _g ⁻ e	3Σ _g ⁻ (2s _g ² 2s _u ² 2π _u ²)	V ₂ (V7.5-s2p2d2)	1Σ ⁺ _g ⁺ n	1Σ ⁺ _g ⁺ (4sσ _g ² 3dσ _g ² 3dπ _u ⁴ 3dδ _g ²)
C ₂ (C5.0-s2p2)	1Σ ⁺ _g ⁺ f	1Σ ⁺ _g ⁺ (2s _g ² 2s _u ² 2pπ _u ⁴)	V ₂ (V7.5-s4p4d4f2)	3Σ _g ⁻ n	3Σ _g ⁻ (4sσ _g ² 3dσ _g ² 3dπ _u ⁴ 3dδ _g ²)
N ₂ (N5.0-s2p2)	1Σ ⁺ _g ⁺ f	1Σ ⁺ _g ⁺ (2s _g ² 2pπ _u ⁴ 2pσ _g ²)	Cr ₂ (Cr7.0-s2p2d2)	1Σ ⁺ _g ⁺ o	1Σ ⁺ _g ⁺ (4sσ _g ² 3dσ _g ² 3dπ _u ⁴ 3dδ _g ⁴)
O ₂ (O5.0-s2p2)	3Σ _g ⁻ f	3Σ _g ⁻ (2pσ _g ² 2pπ _u ⁴ 2pπ _g ²)	MnO (Mn7.0-s2p2d2)	6Σ ⁺ _g ⁺ p	6Σ ⁺ _g ⁺ (dσ ¹ dπ ⁴ dδ ² dπ*2)
F ₂ (F5.0-s2p2)	1Σ ⁺ _g ⁺ f	1Σ ⁺ _g ⁺ (2pσ _g ² 2pπ _u ⁴ 2pπ _g ⁴)	Fe ₂ (Fe7.0-s2p2d2)	7Δ _u ⁺ q	7Δ _u ⁺ (4sσ _g ² 3dσ _g ² 3dσ _u ¹ 3dπ _u ⁴ 3dπ _g ⁴ 3dδ _g ³ 3dδ _u ²)
Ne ₂ (Ne7.0-s2p2)	1Σ ⁺ _g ⁺ g	1Σ ⁺ _g ⁺ (2pπ _u ⁴ 2pσ _g ² 2pσ _u ²)	Co ₂ (Co7.0-s2p2d2)	5Δ _g ⁺	5Δ _g ⁺ (4sσ _g ² 3dσ _g ² 3dσ _u ¹ 3dπ _u ⁴ 3dπ _g ⁴ 3dδ _g ⁴ 3dδ _u ³)
Na ₂ (Na9.0-s2p2)	1Σ ⁺ _g ⁺ f	1Σ ⁺ _g ⁺ (2pπ _u ⁴ 2pσ _g ² 3sσ _g ²)	Ni ₂ (Ni7.0-s2p2d2)	Ω ^r	3Σ _g ⁻ (4sσ _g ² 3dσ _g ² 3dσ _u ¹ 3dπ _u ⁴ 3dπ _g ⁴ 3dδ _g ⁴ 3dδ _u ⁴)
MgO (Mg7.0-s2p2)	1Σ ⁺ _g ⁺ h	1Σ ⁺ _g ⁺ (sσ ² sσ ² pπ ⁴)	Cu ₂ (Cu7.0-s2p2d2)	1Σ ⁺ _g ⁺ s	1Σ ⁺ _g ⁺ (4sσ _g ² 3dσ _g ² 3dσ _u ¹ 3dπ _u ⁴ 3dπ _g ⁴ 3dδ _g ⁴ 3dδ _u ⁴)
Al ₂ (Al6.5-s2p2)	3Π _u ⁻ i	3Σ _g ⁻ (3sσ _g ² 3sσ _u ² 3pπ _u ²)	ZnH (Zn7.0-s2p2d2)	2Σ ⁺ _g ⁺ t	2Σ ⁺ _g ⁺ (sσ ² sσ*1dσ ² dπ ⁴ dδ ⁴)
Al ₂ (Al6.5-s4p4d2)	3Π _u ⁻ i	3Σ _g ⁻ (3sσ _g ² 3sσ _u ² 3pπ _u ²)	GaH (Ga7.0-s2p2)	1Σ ⁺ _g ⁺ u	1Σ ⁺ _g ⁺ (sσ ² sσ*2)
Si ₂ (Si6.5-s2p2)	3Σ _g ⁻ f	3Π _u ⁻ (3sσ _g ² 3sσ _u ¹ 3pπ _u ³)	GeO (Ge7.0-s2p2)	1Σ ⁺ _g ⁺ f	1Σ ⁺ _g ⁺ (ssσ ² spo ² ppπ ⁴ ppσ ²)
Si ₂ (Si6.5-s2p2d1)	3Σ _g ⁻ f	3Σ _g ⁻ (3sσ _g ² 3pπ _u ² 3sσ _u ²)	As ₂ (As7.0-s2p2d1)	1Σ ⁺ _g ⁺ f	1Σ ⁺ _g ⁺ (4sσ _g ² 4sσ _u ² 4pσ _g ² 4pπ _u ⁴)
P ₂ (P6.0-s2p2d1)	1Σ ⁺ _g ⁺ f	1Σ ⁺ _g ⁺ (3sσ _g ² 3pσ _g ² 3pπ _u ⁴)	Se ₂ (Se7.0-s2p2d1)	3Σ _g ⁻ f	3Σ _g ⁻ (4sσ _g ² 4sσ _u ² 4pσ _g ² 4pπ _u ⁴ 4pπ _g ²)
S ₂ (S6.0-s2p2)	3Σ _g ⁻ f	3Σ _g ⁻ (3pσ _g ² 3pπ _u ⁴ 3pπ _g ²)	Br ₂ (Br7.0-s2p2d1)	1Σ ⁺ _g ⁺ f	1Σ ⁺ _g ⁺ (4sσ _g ² 4sσ _u ² 4pσ _g ² 4pπ _u ⁴ 4pπ _g ⁴)
Cl ₂ (Cl6.0-s2p2d2)	1Σ ⁺ _g ⁺ f	1Σ ⁺ _g ⁺ (3pσ _g ² 3pπ _u ⁴ 3pπ _g ²)	Kr ₂ (Kr7.0-s2p2)	1Σ ⁺ _g ⁺ v	1Σ ⁺ _g ⁺ (4sσ _g ² 4sσ _u ² 4pσ _g ² 4pπ _u ⁴ 4pπ _g ⁴)
Ar ₂ (Ar7.0-s2p2)	1Σ ⁺ _g ⁺ j	1Σ ⁺ _g ⁺ (3pπ _u ⁴ 3pπ _g ² 3pσ _u ²)			

All the successes and failures by the LDA are reproduced by the modest size of basis functions (DNP in most cases).

Accuracy:

Equilibrium bond length of molecules

MAE for expt. 0.067 Å

MAE for other calc. 0.033 Å

PRB 69, 195113 (2004)

	Expt.	OpenMX	Other calc.	Expt.	OpenMX	Other calc.
H ₂	0.741 ^a	0.768	0.766 ^b	K ₂	3.620	3.670 ^b
He ₂	2.97 ^c	2.417	2.397 ^d	CaO	1.768	1.79 ^h
Li ₂	2.673 ^a	2.748	2.699 ^b	ScO	1.719	1.649 ^b
BeO	1.331 ^a	1.339	1.319 ^e	Ti ₂	1.942 ^m	-
B ₂	1.590 ^a	1.603		V ₂	1.77 ⁿ	1.802 ^o
C ₂	1.243 ^a	1.255	1.249 ^f	Cr ₂	1.679 ^p	1.632 ^q
N ₂	1.098 ^a	1.104	1.094 ^b	MnO	1.648 ^r	1.585 ^b
O ₂	1.208 ^a	1.201	1.197 ^g	Fe ₂	2.02 ^s	1.963 ^t
F ₂	1.412 ^a	1.435	1.388 ^b	Co ₂	-	1.93 ^u
Ne ₂	3.09 ^c	2.692	2.641 ^d	Ni ₂	2.155 ^v	2.037 ^w
Na ₂	3.079 ^a	3.140	3.048 ^b	Cu ₂	2.220 ^a	2.170 ^w
MgO	1.749 ^a	1.770	1.76 ^h	ZnH	1.595 ^a	1.593 ^b
Al ₂	2.650 ⁱ	2.710	2.73 ^j	GaH	1.663 ^a	1.681 ^b
Si ₂	2.246 ^a	2.281	2.280 ^k	GeO	1.625 ^a	1.593 ^b
P ₂	1.893 ^a	1.926	1.877 ^b	As ₂	2.103 ^a	2.070 ^b
S ₂	1.889 ^a	1.936	1.942 ^l	Se ₂	2.166 ^a	2.164 ^b
Cl ₂	1.987 ^a	1.946	1.971 ^b	Br ₂	2.281 ^a	2.273 ^b
Ar ₂	3.76 ^c	3.425	3.42 ^d	Kr ₂	3.951 ^c	3.715 ^d

Accuracy:

Equilibrium lattice constant and bulk modulus of bulks

M/MN	Lattice parameter (Å)	Bulk modulus (GPa)
Al (fcc)	$a_c = 4.05$ $a_r = 4.049$ [76]	$B_c = 79.4$ $B_r = 75.2$ [77]
Cr (bcc)	$a_c = 2.92$ $a_r = 2.895$ [76]	$B_c = 156.8$ $B_r = 160$ [77]
Y (hcp)	$a_c = 3.63$ ($c/a = 1.55$) $a_r = 3.647$ ($c/a = 1.57$) [76]	$B_c = 47.4$ $B_r = 41.2$ [77]
AlN (fcc)	$a_c = 4.13$ $a_r = 4.045, 4.12$ [76], 4.094 [40]	$B_c = 262.2$ $B_r = 174-329$ [78], 252 [18]
AlN (hcp)	$a_c = 3.18$ ($c/a = 1.61$) $a_r = 3.11$ ($c/a = 1.60$) [76], 3.157 [79]	$B_c = 198.1$ $B_r = 185-208$ [18,61,80]
CrN (fcc) (AFM)	$a_c = 4.22$ $a_r = 4.148$ [76], 4.162 [81], 4.185 [82], 4.206 [40]	$B_c = 277.7$ $B_r = 245$ [18]
CrN (hcp)	$a_c = 3.19$ ($c/a = 1.62$) $a_r = 3.111$ ($c/a = 1.64$) [18]	$B_c = 185.6$ $B_r = 188$ [18]
YN (fcc)	$a_c = 4.99$ $a_r = 4.76-4.93$ [83], 4.89 [76]	$B_c = 151.4$ $B_r = 145-187$ [83]
YN (hcp)	$a_c = 3.83$ ($c/a = 1.57$) $a_r = 3.67 - 3.78$ ($c/a = 1.58-1.62$) [83]	$B_c = 112.6$ $B_r = 110-139$ [83]

F. Rovere, D. Music, J.M. Schneider, and P.H. Mayrhofer, Acta Materialia 58, 2708 (2010).

The lattice constants are reproduced within **error of 1 %** compared to other calculations and experimental results.

The bulk moduli are reproduced within **error of 15 %** compared to other calculations and experimental results.

When we go beyond LDA

Although LB is not a systematic basis, it can be a practical platform when we go beyond LDA and GGA, where non-local functionals such as the Hartree-Fock exchange are involved.

In the case, the large number of basis functions in the other methods may cause difficulty in the actual applications.

Points of concern for reliable & efficient calculations

- ✓ **Choice of basis functions**
- ✓ Numerical grid for E_{tot}
- ✓ Quality of pseudopotentials

Basis functions in OpenMX

1) Primitive functions

generated by a confinement scheme

2) Optimized functions

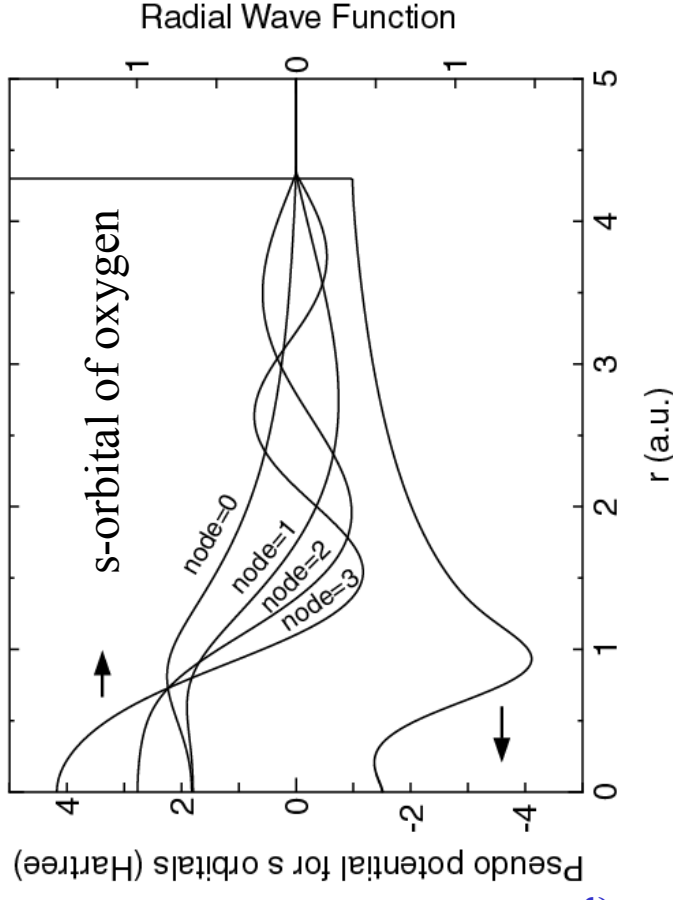
by an orbital optimization method

Primitive basis functions

1. Solve an atomic Kohn-Sham eq. under a confinement potential:

$$V_{\text{core}}(r) = \begin{cases} -\frac{Z}{r} & \text{for } r \leq r_1 \\ \sum_{n=0}^3 b_n r^n & \text{for } r_1 < r \leq r_c \\ h & \text{for } r_c < r, \end{cases}$$

2. Construct the norm-conserving pseudopotentials.
3. Solve ground and excited states for the pseudopotentials.

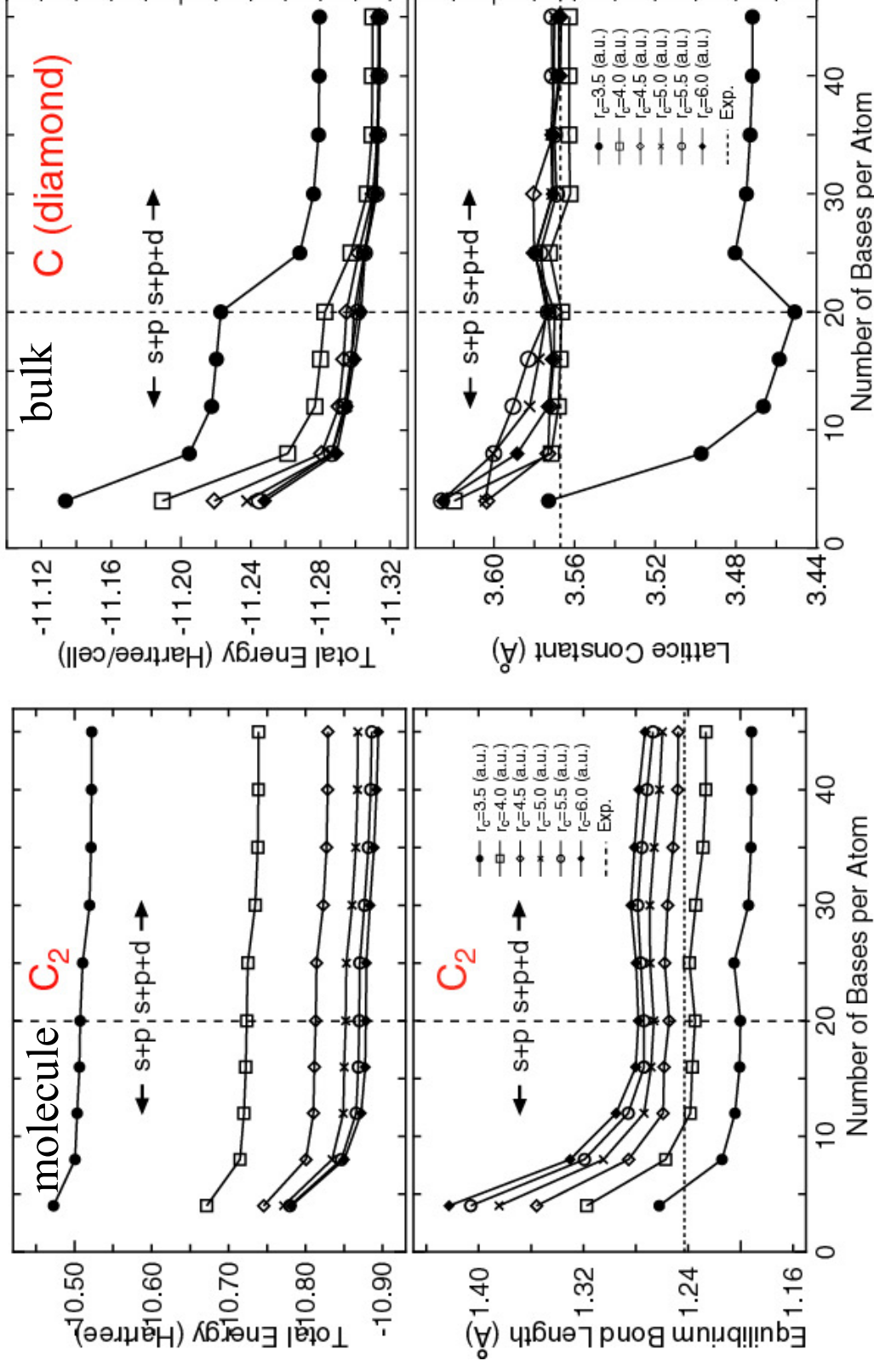


In most cases, the accuracy and efficiency can be controlled by

Cutoff radius
Number of orbitals

Convergence with respect to basis functions

The two parameters can be regarded as variational parameters.



Benchmark of primitive basis functions

Ground state calculations of dimer using primitive basis functions

Dimer	Expt.	Calc.	Dimer	Expt.	Calc.
H ₂ (H4.5-s2)	1Σ ⁺ a	1Σ ⁺ (1s _g ²)	K ₂ (K10.0-s2p2)	1Σ ⁺ f	(3pπ _g ⁴ 3pσ _u ² 4sσ _g ²)
He ₂ (He7.0-s2)	1Σ ⁺ b	1Σ ⁺ (1s _g ² 1s _u ²)	CaO (Ca7.0-s2p2d2)	1Σ ⁺ k	(sσ _g ² sσ _u ² pπ ⁴)
Li ₂ (Li8.0-s2)	1Σ ⁺ c	1Σ ⁺ (2s _g ²)	ScO (Sc7.0-s2p2d2)	2Σ ⁺ l	(dπ ⁴ sσ _g ² sσ _u ²)
BeO (Be6.0-s2p2)	1Σ ⁺ d	1Σ ⁺ (sσ _g ² sσ _u ² pπ ⁴)	Ti ₂ (Ti7.0-s2p2d2)	3Δ _g m	(4sσ _g ² 3dσ _g ¹ 3dπ _u ⁴ 3dδ _u ¹)
B ₂ (B5.5-s2p2)	3Σ _g ⁻ e	3Σ _g ⁻ (2sσ _g ² 2sσ _u ² 2π _u ²)	V ₂ (V7.5-s2p2d2)	1Σ ⁺ n	(4sσ _g ² 3dσ _g ² 3dπ _u ⁴ 3dδ _g ²)
C ₂ (C5.0-s2p2)	1Σ ⁺ f	1Σ ⁺ (2sσ _g ² 2sσ _u ² 2pπ _u ⁴)	V ₂ (V7.5-s4p4d4f2)	3Σ _g ⁻ n	(4sσ _g ² 3dσ _g ² 3dπ _u ⁴ 3dδ _g ²)
N ₂ (N5.0-s2p2)	1Σ ⁺ f	1Σ ⁺ (2sσ _g ² 2pπ _u ⁴ 2pσ _g ²)	Cr ₂ (Cr7.0-s2p2d2)	1Σ ⁺ o	(4sσ _g ² 3dσ _g ² 3dπ _u ⁴ 3dδ _u ¹)
O ₂ (O5.0-s2p2)	3Σ _g ⁻ f	3Σ _g ⁻ (2pσ _g ² 2pπ _u ⁴ 2pπ _g ²)	MnO (Mn7.0-s2p2d2)	6Σ ⁺ p	(dσ _g ¹ dπ ⁴ dδ ² dπ ^{*2})
F ₂ (F5.0-s2p2)	1Σ ⁺ f	1Σ ⁺ (2pσ _g ² 2pπ _u ⁴ 2pπ _g ⁴)	Fe ₂ (Fe7.0-s2p2d2)	7Δ _u q	(4sσ _g ² 3dσ _g ² 3dσ _u ¹ 3dπ _u ⁴ 3dπ _g ² 3dδ _g ² 3dδ _u ²)
Ne ₂ (Ne7.0-s2p2)	1Σ ⁺ g	1Σ ⁺ (2pπ _u ⁴ 2pπ _g ⁴ 2pσ _u ²)	Co ₂ (Co7.0-s2p2d2)	5Δ _g	(4sσ _g ² 3dσ _g ² 3dσ _u ¹ 3dπ _u ⁴ 3dπ _g ² 3dδ _g ⁴ 3dδ _u ²)
Na ₂ (Na9.0-s2p2)	1Σ ⁺ f	1Σ ⁺ (2pπ _g ⁴ 2pσ _g ² 3sσ _g ²)	Ni ₂ (Ni7.0-s2p2d2)	Ω r	(4sσ _g ² 3dσ _g ² 3dσ _u ² 3dπ _u ⁴ 3dπ _g ² 3dδ _g ⁴ 3dδ _u ⁴)
MgO (Mg7.0-s2p2)	1Σ ⁺ h	1Σ ⁺ (sσ _g ² sσ _u ² pπ ⁴)	Cu ₂ (Cu7.0-s2p2d2)	1Σ ⁺ s	(4sσ _g ² 3dσ _g ² 3dσ _u ² 3dπ _u ⁴ 3dπ _g ² 3dδ _g ⁴ 3dδ _u ⁴)
Al ₂ (Al6.5-s2p2)	3Π _u i	3Σ _g ⁻ (3sσ _g ² 3sσ _u ² 3pπ _u ²)	ZnH (Zn7.0-s2p2d2)	2Σ ⁺ t	(sσ _g ² sσ _u ² dσ _g ² dπ ⁴ dδ ⁴)
Al ₂ (Al6.5-s4p4d2)	3Π _u i	3Σ _g ⁻ (3sσ _g ² 3sσ _u ² 3pπ _u ²)	GaH (Ga7.0-s2p2)	1Σ ⁺ u	(sσ _g ² sσ _u ²)
Si ₂ (Si6.5-s2p2)	3Σ _g ⁻ f	3Π _u (3sσ _u ² 3sσ _g ¹ 3pπ _u ³)	GeO (Ge7.0-s2p2)	1Σ ⁺ f	(ssσ _g ² spo _g ² ppπ ⁴ ppσ _g ²)
Si ₂ (Si6.5-s2p2d1)	3Σ _g ⁻ f	3Σ _g ⁻ (3sσ _u ² 3pπ _u ² 3sσ _g ²)	As ₂ (As7.0-s2p2d1)	1Σ ⁺ f	(4sσ _g ² 4sσ _u ² 4pσ _g ² 4pπ _u ⁴)
P ₂ (P6.0-s2p2d1)	1Σ ⁺ f	1Σ ⁺ (3sσ _u ² 3pσ _g ² 3pπ _u ⁴)	Se ₂ (Se7.0-s2p2d1)	3Σ _g ⁻ f	(4sσ _g ² 4sσ _u ² 4pσ _g ² 4pπ _u ⁴ 4pπ _g ²)
S ₂ (S6.0-s2p2)	3Σ _g ⁻ f	3Σ _g ⁻ (3pσ _g ² 3pπ _u ⁴ 3pπ _g ²)	Br ₂ (Br7.0-s2p2d1)	1Σ ⁺ f	(4sσ _g ² 4sσ _u ² 4pσ _g ² 4pπ _u ⁴ 4pπ _g ⁴)
Cl ₂ (Cl6.0-s2p2d2)	1Σ ⁺ f	1Σ ⁺ (3pσ _g ² 3pπ _u ⁴ 3pπ _g ⁴)	Kr ₂ (Kr7.0-s2p2)	1Σ ⁺ v	(4sσ _g ² 4sσ _u ² 4pσ _g ² 4pσ _u ² 4pπ _u ⁴ 4pπ _g ⁴)
Ar ₂ (Ar7.0-s2p2)	1Σ ⁺ j	1Σ ⁺ (3pπ _u ⁴ 3pπ _g ⁴ 3pσ _u ²)			

All the successes and failures by the LDA are reproduced by the modest size of basis functions (DNP in most cases)

Optimization of basis functions

Practically, the accuracy and efficiency can be controlled by

Number of basis functions

Cutoff radius

But, there is another one variational parameter:

Radial shape

If the radial shape can be optimized, it is expected that the high accuracy will be attainable with a small number of basis functions.

Variational optimization of basis functions No.1

One-particle wave functions

$$\psi_{\mu}(\mathbf{r}) = \sum_{i\alpha} c_{\mu,i\alpha} \phi_{i\alpha}(\mathbf{r} - \mathbf{r}_i),$$

Contracted orbitals

$$\phi_{i\alpha}(\mathbf{r}) = \sum_q a_{i\alpha q} \chi_{i\eta}(\mathbf{r}),$$

The variation of E with respect to \mathbf{c} with fixed \mathbf{a} gives

$$\frac{\partial E_{\text{tot}}}{\partial a} = 0 \quad \sum_{j\beta} \langle \phi_{i\alpha} | \hat{H} | \phi_{j\beta} \rangle c_{\mu,j\beta} = \epsilon_{\mu} \sum_{j\beta} \langle \phi_{i\alpha} | \phi_{j\beta} \rangle c_{\mu,j\beta},$$

Regarding \mathbf{c} as dependent variables on \mathbf{a} and assuming KS eq. is solved self-consistently with respect to \mathbf{c} , we have

$$\begin{aligned} \frac{\partial E_{\text{tot}}}{\partial a_{i\alpha q}} &= \frac{\delta E_{\text{tot}}}{\delta \rho(\mathbf{r})} \frac{\delta \rho(\mathbf{r})}{\delta a_{i\alpha q}} \\ &= 4 \sum_{\mu} n_{\mu} \sum_{i\alpha,j\beta} c_{\mu,i\alpha} c_{\mu,j\beta} \left\langle \frac{\partial \phi_{i\alpha}}{\partial a_{i\alpha q}} | \hat{H} | \phi_{j\beta} \right\rangle + 4 \sum_{\mu} n_{\mu} \sum_{i\alpha,j\beta} \frac{\partial c_{\mu,i\alpha}}{\partial a_{i\alpha q}} c_{\mu,j\beta} \langle \phi_{i\alpha} | \hat{H} | \phi_{j\beta} \rangle \\ &= 2 \sum_{j\beta} \left(\Theta_{i\alpha,j\beta} \langle \chi_{i\eta} | \hat{H} | \phi_{j\beta} \rangle - E_{i\alpha,j\beta} \langle \chi_{i\eta} | \phi_{j\beta} \rangle \right), \end{aligned}$$

Variational optimization of basis functions No.2

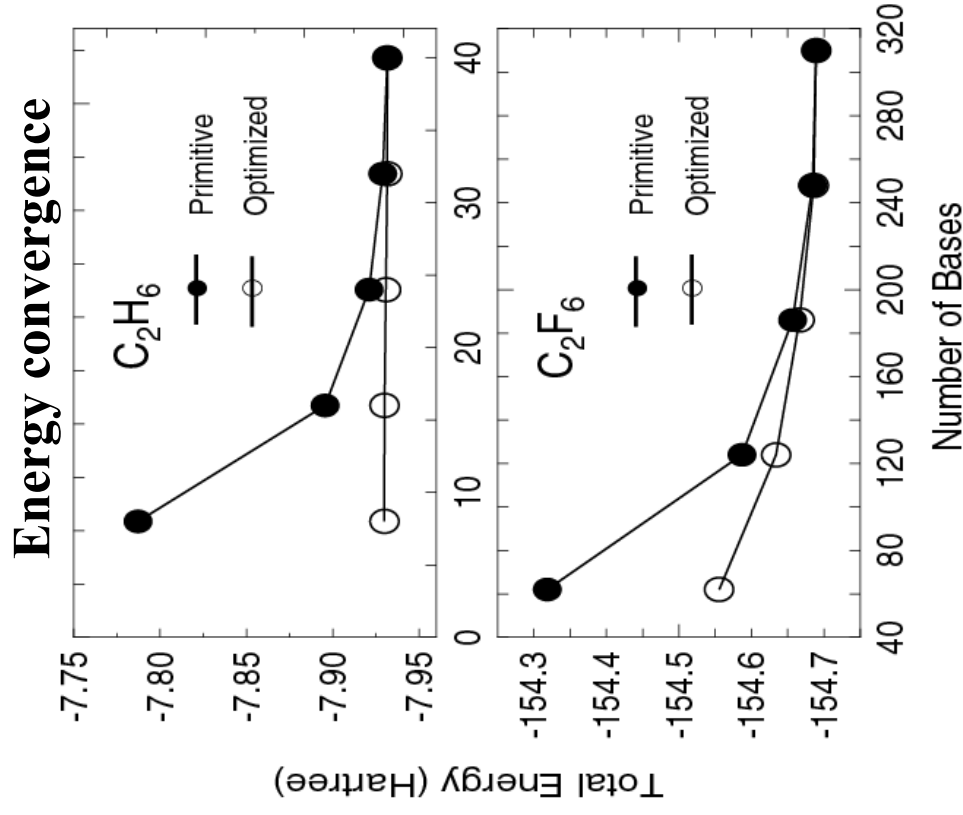
The basis functions can be optimized in the same procedure as for the geometry optimization.

Step 1 Self-consistently solving of Eq. (4),

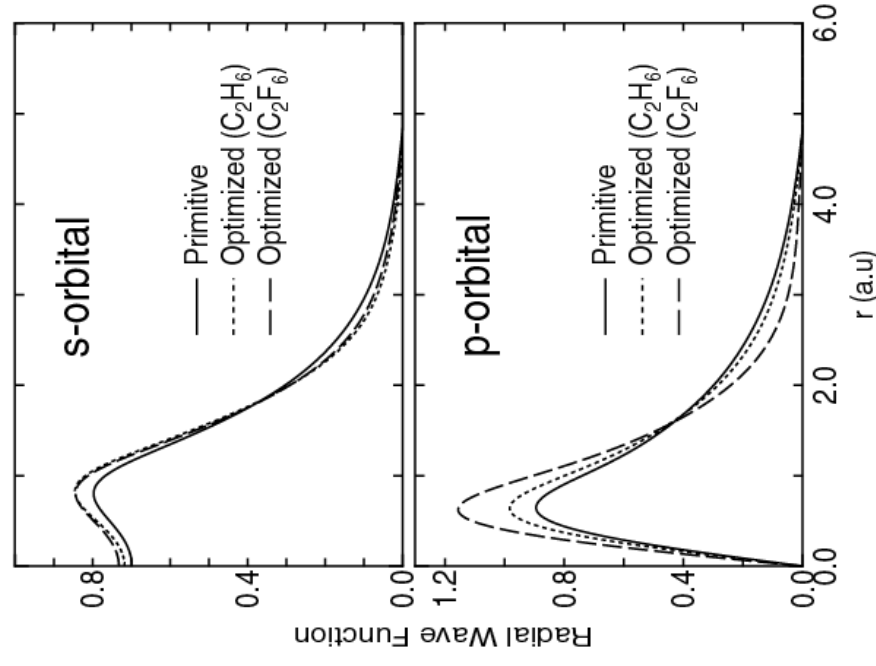
$$\text{Step 2 } a_{i\alpha q}^{(n+1)} = a_{i\alpha q}^{(n)} - \lambda \left(\frac{\partial E_{\text{tot}}}{\partial a_{i\alpha q}} \right)_{a^{(n)}},$$

$$n := n + 1,$$

Primitive vs. Optimized



Radial shape of carbon atom



Since the fluorine attracts electrons sitting p-orbitals of carbon, the p-orbital of carbon largely shrinks.

Points of concern for reliable & efficient calculations

- ✓ Choice of basis functions
- ✓ Numerical grid
- ✓ Quality of pseudopotentials

When you calculate a system consisting of elements A, B, and C, it would be better to start from calculations of elemental systems of A, B and C, which can be easily compared to published results and other codes. These calculations give us a guideline for how large basis functions should be used for these elements. Otherwise, it is difficult to say whether your calculations are reliable or not.

Possible choice of basis functions

The proper choice of basis functions depends on elements and chemical environment. Although detailed analyses can be found in PRB 69, 195113 (2004) and JCP 121, 10879 (2004), the following can be good starting points.

Examples	H4.5-s2	Li8.0-s2	Ti5.5-s2p2d1	Fe5.5-s2p2d1
	B4.5-s2p1	Na9.0-s2	V5.5-s2p2d1	Co5.5-s2p2d1
	C4.5-s2p1	K9.0-s2	Cr5.5-s2p2d1	Ni5.5-s2p2d1
	N4.5-s2p2		Mn5.5-s2p2d1	Cu5.5-s2p2d1
	O4.5-s2p2d1			
	F4.5-s2p2d1			

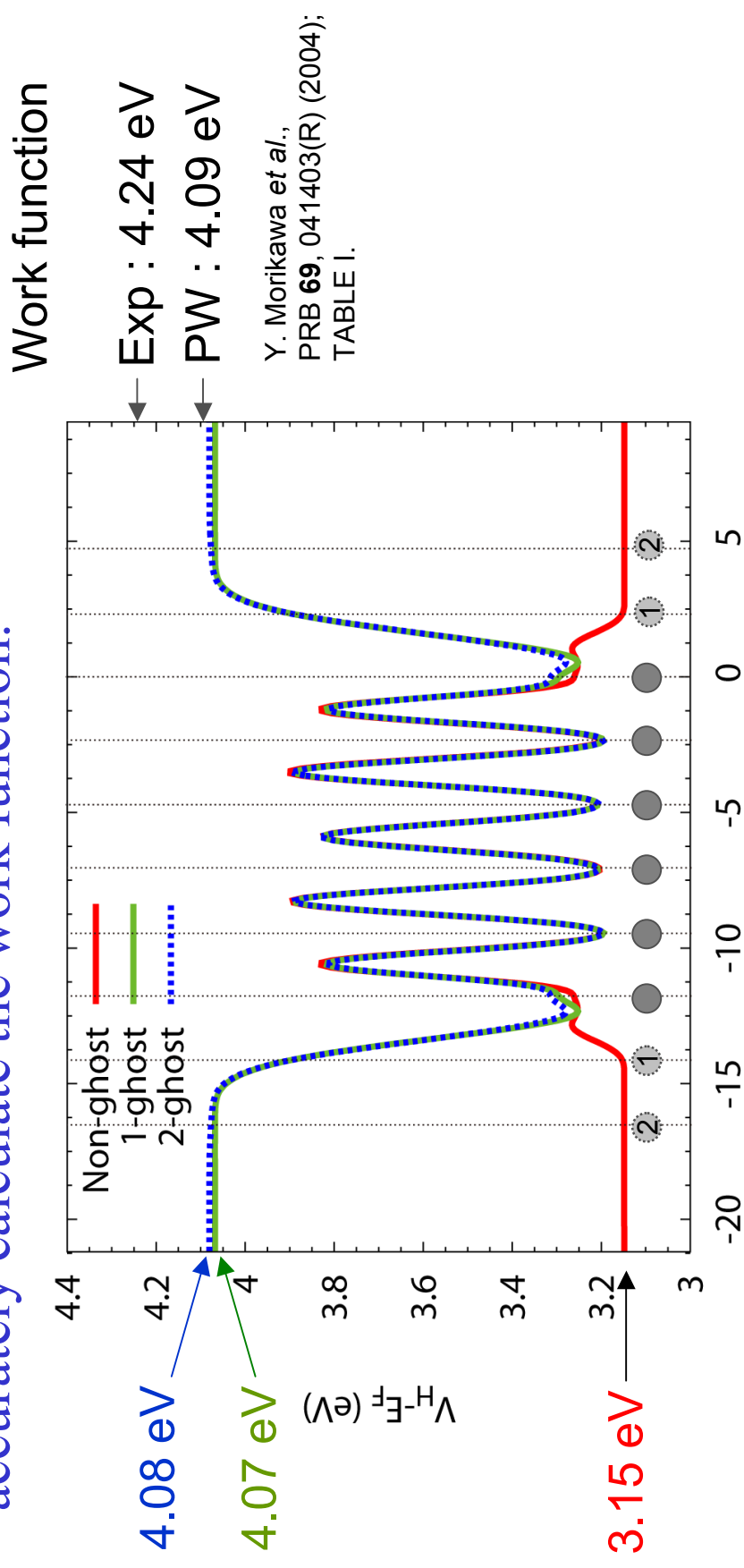
Trends:

- (1) Elements located in the right side of the periodic table require basis sets with higher angular momentum.
- (2) Alkali metals require a long tail of basis functions.
- (3) 3d-transition metals are well described by TM5.5-s2p2d1 in their oxide.

Treatment of surface

Work function of fcc Al (111) surface

The use of basis functions in the ghost layers is crucial to accurately calculate the work function.



Coordinate along the surface normal (Ang.)

By Jippo and Ohfuti (Fujitsu)

Al(111) fcc 1x1 6L, GGA-PBE, Fix to the equilibrium lattice parameter
Al6.0-s1p2d1, Al_PBE (Database ver. 2006)
E6.0-s1p2d1, E (Database ver. 2006)

Atomization energy:BSSE

H₂ molecule (Expt. 4.5 eV)

H4.0-s1 H4.0-s2 H5.5-s4

Atomization
Energy (eV)

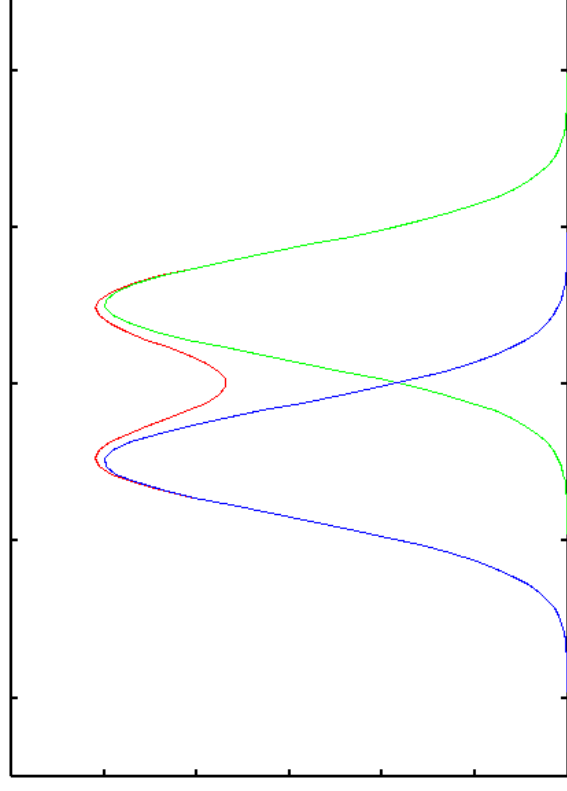
4.89 5.35 4.88

Corrected by
counterpoise
method (eV)

4.68 5.18 4.85

BSSE (eV)
(Basis set
superposition
error)

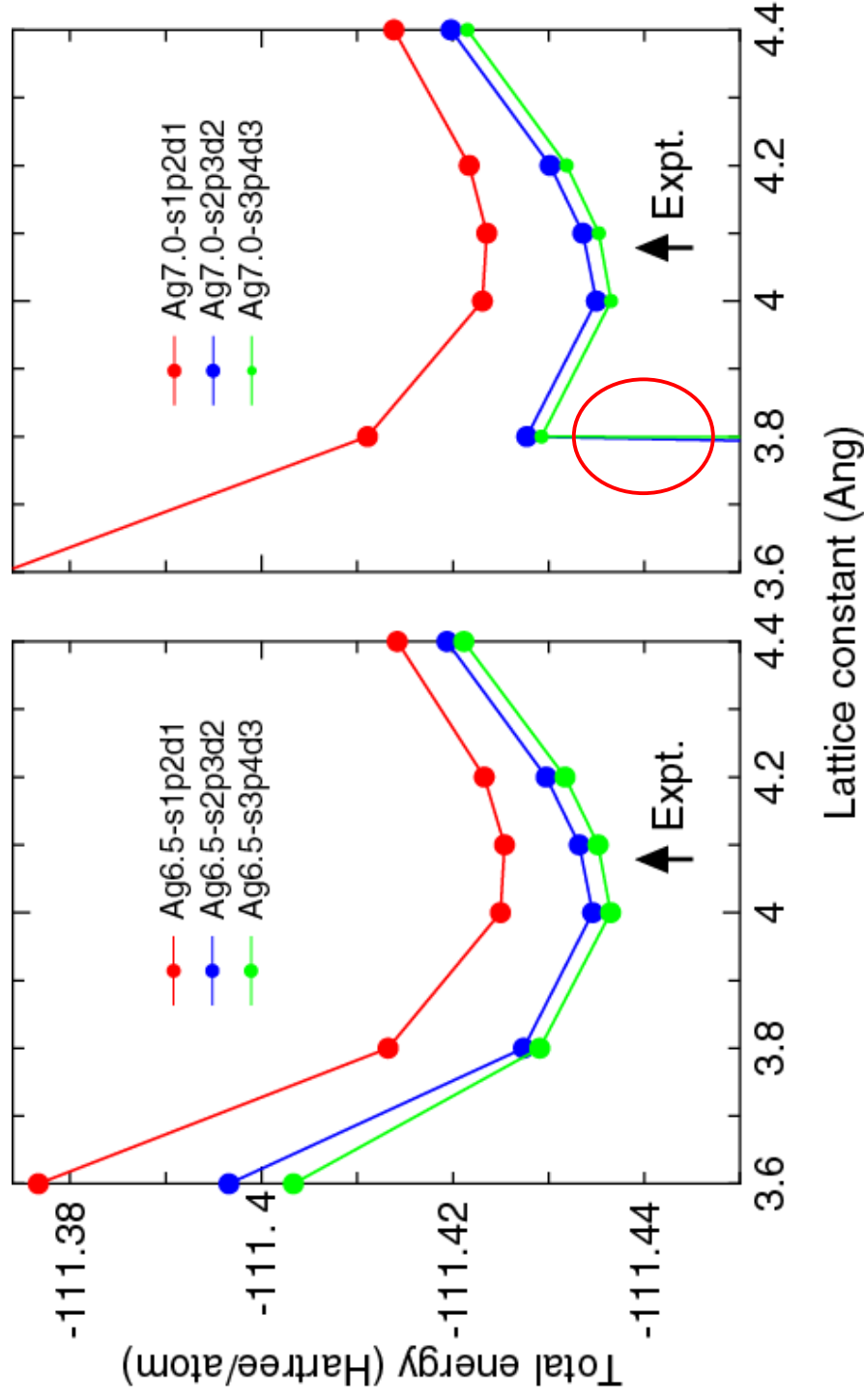
0.21 0.17 0.03



In molecules and bulks, wave functions around certain atom are expressed by basis functions of neighboring atoms. The effect increases the atomization energy. **The counterpoise scheme is a prescription.**

Overcompleteness

Total energy curves of fcc-Ag



For dense structures such as fcc, hcp, and bcc, a large basis set tends to cause a numerical instability known as overcompleteness.

Points of concern for reliable & efficient calculations

- ✓ Choice of basis functions
- ✓ **Numerical grid for E_{tot}**
- ✓ Quality of pseudopotentials

Total energy No.1

The total energy is given by that of the conventional DFT. The reorganization of the Coulomb energies is a key for the accurate implementation

$$E_{\text{tot}} = E_{\text{kin}} + E_{\text{ec}} + E_{\text{ee}} + E_{\text{xc}} + E_{\text{cc}}.$$

$$E_{\text{kin}} = \sum_{\sigma} \sum_{\frac{N}{n}} \sum_{i\alpha, j\beta}^{(\mathbf{R}_n)} \rho_{\sigma, i\alpha j\beta} h_{i\alpha j\beta, \text{kin}}^{(\mathbf{R}_n)}.$$

$$E_{\text{ec}} = E_{\text{ec}}^{(\text{L})} + E_{\text{ec}}^{(\text{NL})},$$

$$= \sum_{\sigma} \sum_{\frac{N}{n}} \sum_{i\alpha, j\beta}^{(\mathbf{R}_n)} \rho_{\sigma, i\alpha j\beta} \langle \phi_{i\alpha}(\mathbf{r} - \tau_i) | \sum_I V_{\text{core}, I}(\mathbf{r} - \tau_I) | \phi_{j\beta}(\mathbf{r} - \tau_j - \mathbf{R}_n) \rangle$$

$$+ \sum_{\sigma} \sum_{\frac{N}{n}} \sum_{i\alpha, j\beta}^{(\mathbf{R}_n)} \rho_{\sigma, i\alpha j\beta} \langle \phi_{i\alpha}(\mathbf{r} - \tau_i) | \sum_I V_{\text{NL}, I}(\mathbf{r} - \tau_I) | \phi_{j\beta}(\mathbf{r} - \tau_j - \mathbf{R}_n) \rangle,$$

$$E_{\text{ee}} = \frac{1}{2} \int d\mathbf{r}^3 n(\mathbf{r}) V_{\text{H}}(\mathbf{r}),$$

$$= \frac{1}{2} \int d\mathbf{r}^3 n(\mathbf{r}) \{ V_{\text{H}}^{(\text{a})}(\mathbf{r}) + \delta V_{\text{H}}(\mathbf{r}) \},$$

$$E_{\text{xc}} = \int d\mathbf{r}^3 \{ n_{\uparrow}(\mathbf{r}) + n_{\downarrow}(\mathbf{r}) + n_{\text{pcc}}(\mathbf{r}) \} \epsilon_{\text{xc}}(n_{\uparrow} + \frac{1}{2}n_{\text{pcc}}, n_{\downarrow} + \frac{1}{2}n_{\text{pcc}}),$$

$$E_{\text{cc}} = \frac{1}{2} \sum_{I, J} \frac{Z_I Z_J}{|\tau_I - \tau_J|}.$$

Total energy No.2

The reorganization of Coulomb energies gives **three new energy terms**.

$$E_{\text{ec}}^{(L)} + E_{\text{ee}} + E_{\text{cc}} = E_{\text{na}} + E_{\delta\text{ee}} + E_{\text{ecc}},$$

The neutral atom energy

$$\begin{aligned} E_{\text{na}} &= \int dr^3 n(\mathbf{r}) \sum_I V_{\text{na},I}(\mathbf{r} - \tau_I), \\ &= \sum_{\sigma} \sum_{\mathbf{n}} \sum_{i\alpha,j\beta} \rho_{\sigma,i\alpha,j\beta}^{(\mathbf{R}_{\mathbf{n}})} \sum_I \langle \phi_{i\alpha}(\mathbf{r} - \tau_i) | V_{\text{na},I}(\mathbf{r} - \tau_I) | \phi_{j\beta}(\mathbf{r} - \tau_j - \mathbf{R}_{\mathbf{n}}) \rangle, \end{aligned}$$

Difference charge Hartree energy

$$E_{\delta\text{ee}} = \frac{1}{2} \int dr^3 \delta n(\mathbf{r}) \delta V_{\text{H}}(\mathbf{r}),$$

Screened core-core repulsion energy

$$E_{\text{scc}} = \frac{1}{2} \sum_{I,J} \left[\frac{Z_I Z_J}{|\tau_I - \tau_J|} - \int dr^3 n_I^{(a)}(\mathbf{r}) V_{\text{H},J}^{(a)}(\mathbf{r}) \right].$$

Difference charge

$$\begin{aligned} \delta n(\mathbf{r}) &= n(\mathbf{r}) - n^{(a)}(\mathbf{r}), \\ &= n(\mathbf{r}) - \sum_i n_i^{(a)}(\mathbf{r}), \end{aligned}$$

Neutral atom potential

$$V_{\text{na},I}(\mathbf{r} - \tau_I) = V_{\text{core},I}(\mathbf{r} - \tau_I) + V_{\text{H},I}^{(a)}(\mathbf{r} - \tau_I).$$

Total energy No.3

So, the total energy is given by

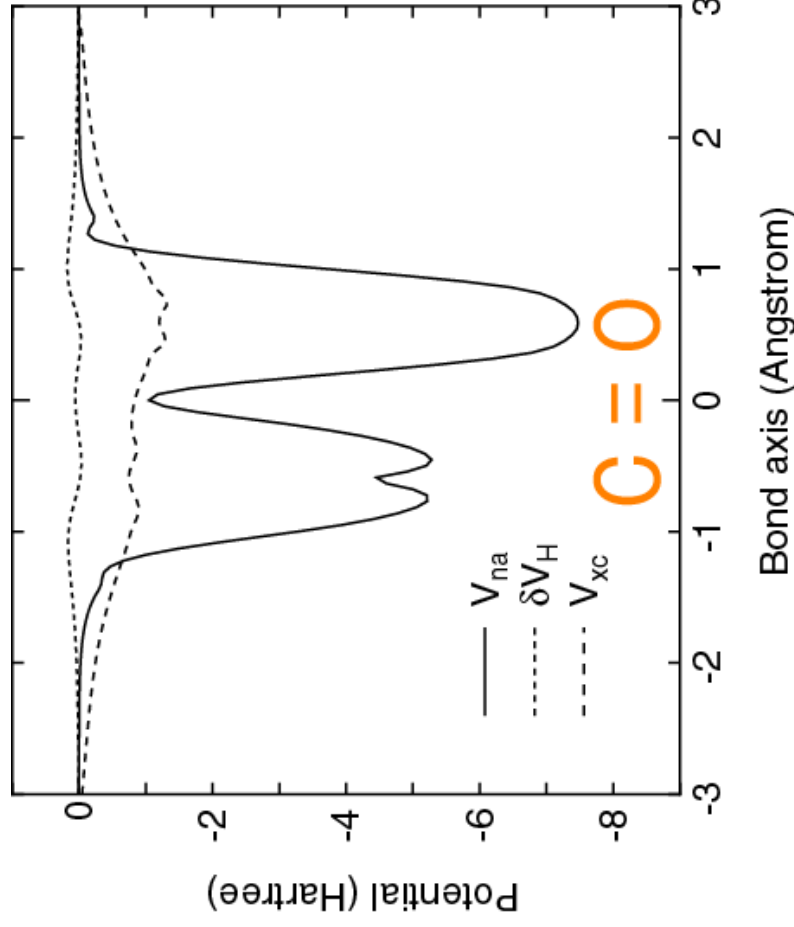
$$E_{\text{tot}} = E_{\text{kin}} + E_{\text{na}} + E_{\text{ec}}^{(\text{NL})} + E_{\delta\text{ee}} + E_{\text{xc}} + E_{\text{scc}}.$$

Each term is evaluated by using a different numerical grid.

E_{kin}	}	Spherical coordinate in momentum space
E_{na}		
$E_{\text{ec}}^{(\text{NL})}$		
$E_{\delta\text{ee}}$	}	Real space regular mesh
E_{xc}		
E_{scc}		Real space fine mesh

Projector expansion of V_{na} No.1

V_{na} tends to be very **deep**, leading to a serious numerical problem.



$$V_{\text{eff}} = \sum_k V_{\text{NL},k} + \sum_k V_{\text{na},k} + \delta V_{\text{H}} + V_{\text{xc}},$$

V_{na} can be expanded by projectors:

$$\hat{V}_{\text{na},k} = \sum_{lm}^{L_{\text{max}}} \sum_{\zeta}^{N_{\text{rad}}} |V_{\text{na},k} \bar{R}_{l\zeta} Y_{lm}\rangle \frac{1}{c_{l\zeta}} \langle Y_{lm} \bar{R}_{l\zeta} V_{\text{na},k} |,$$

where a set of radial functions $\{R_{l\zeta}\}$ is an orthonormal set defined by a norm $\int r^2 dr R_{na,l} k R'$ for radial functions R and R' , and is calculated by the following Gram-Schmidt orthogonalization:

$$\bar{R}_{l\zeta} = R_{l\zeta} - \sum_{\eta}^{\zeta-1} \bar{R}_{l\eta} \frac{1}{c_{l\eta}} \int r^2 dr \bar{R}_{l\eta} V_{\text{na},k} R_{l\zeta},$$

$$c_{l\zeta} = \int r^2 dr \bar{R}_{l\zeta} V_{\text{na},k} \bar{R}_{l\zeta}.$$

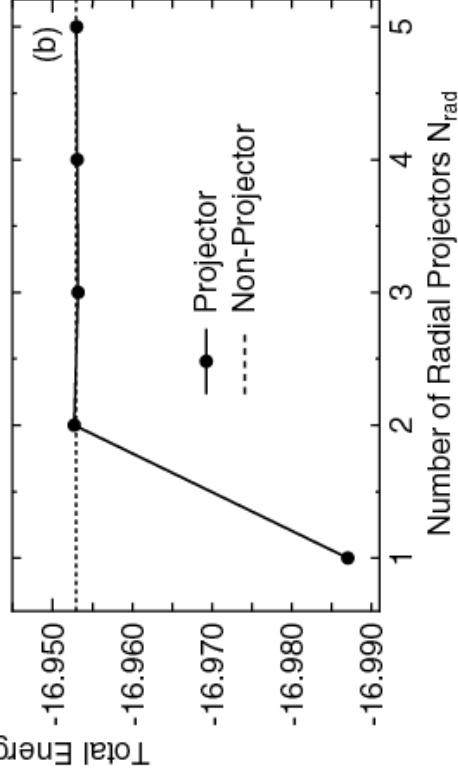
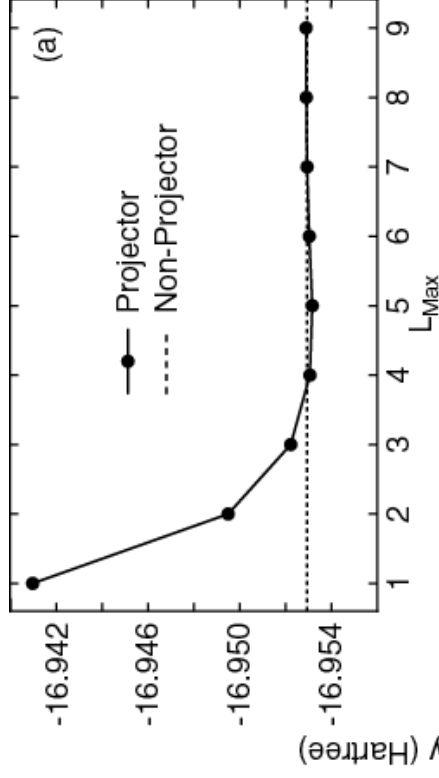
TO and H.Kino, PRB 72, 045121 (2005)

Three center integrals with V_{na} can be transformed to products of two center integrals by the projector expansion method.

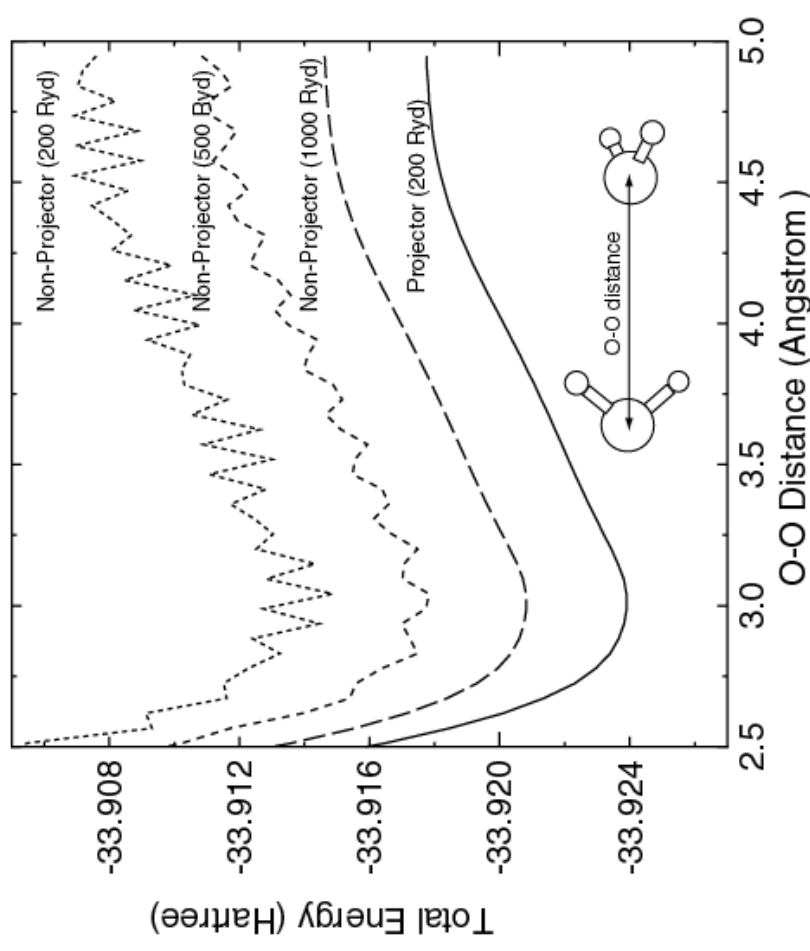
Projector expansion of V_{na} No.2

Convergence properties

$$\hat{V}_{na,k} = \sum_{l_m}^{L_{\max}} \sum_{\zeta}^{N_{\text{rad}}} |V_{na,k} \bar{R}_{l\zeta} Y_{l_m}\rangle \frac{1}{c_{l\zeta}} \langle Y_{l_m} \bar{R}_{l\zeta} V_{na,k} |,$$



Comparison between non-projector and projector methods



Two center integrals

Fourier-transformation of basis functions

$$\begin{aligned}
 \tilde{\phi}_{i\alpha}(\mathbf{k}) &= \left(\frac{1}{\sqrt{2\pi}} \right)^3 \int d\mathbf{r}^3 \phi_{i\alpha}(\mathbf{r}) e^{-i\mathbf{k}\cdot\mathbf{r}} \\
 &= \left(\frac{1}{\sqrt{2\pi}} \right)^3 \int d\mathbf{r}^3 Y_{lm}(\hat{\mathbf{r}}) R_{pl}(\mathbf{r}) \left\{ 4\pi \sum_{L=0}^{\infty} \sum_{M=-L}^L (-i)^L j_L(kr) Y_{LM}(\hat{\mathbf{k}}) Y_{LM}^*(\hat{\mathbf{r}}) \right\}, \\
 &= \left(\frac{1}{\sqrt{2\pi}} \right)^3 4\pi \sum_{L=0}^{\infty} \sum_{M=-L}^L (-i)^L Y_{LM}(\hat{\mathbf{k}}) \int drr^2 R_{pl}(\mathbf{r}) j_L(kr) \int d\theta d\phi \sin(\theta) Y_{lm}(\hat{\mathbf{r}}) Y_{LM}^*(\hat{\mathbf{r}}), \\
 &= \left[\left(\frac{1}{\sqrt{2\pi}} \right)^3 4\pi (-i)^l \int drr^2 R_{pl}(\mathbf{r}) j_L(kr) \right] Y_{lm}(\hat{\mathbf{k}}), \\
 &= \tilde{R}_{pl}(k) Y_{lm}(\hat{\mathbf{k}}),
 \end{aligned}$$

e.g., overlap integral

$$\begin{aligned}
 \langle \phi_{i\alpha}(\mathbf{r}) | \phi_{j\beta}(\mathbf{r} - \boldsymbol{\tau}) \rangle &= \int d\mathbf{r}^3 \phi_{i\alpha}^*(\mathbf{r}) \phi_{j\beta}(\mathbf{r} - \boldsymbol{\tau}), \\
 &= \int d\mathbf{r}^3 \left(\frac{1}{\sqrt{2\pi}} \right)^3 \int dk^3 \tilde{R}_{pl}^*(k) Y_{lm}^*(\hat{\mathbf{k}}) e^{-i\mathbf{k}\cdot\mathbf{r}} \left(\frac{1}{\sqrt{2\pi}} \right)^3 \int dk'^3 \tilde{R}_{p'l'}(k') Y_{l'm'}(\hat{\mathbf{k}}') e^{i\mathbf{k}'\cdot(\mathbf{r}-\boldsymbol{\tau})}, \\
 &= \left(\frac{1}{2\pi} \right)^3 \int dk^3 \int dk'^3 e^{-i\mathbf{k}'\cdot\boldsymbol{\tau}} \tilde{R}_{pl}^*(k) Y_{lm}^*(\hat{\mathbf{k}}) \tilde{R}_{p'l'}(k') Y_{l'm'}(\hat{\mathbf{k}}') \int d\mathbf{r}^3 e^{i(\mathbf{k}'-\mathbf{k})\cdot\mathbf{r}}, \\
 &= \int dk^3 e^{-i\mathbf{k}\cdot\boldsymbol{\tau}} \tilde{R}_{pl}^*(k) Y_{lm}^*(\hat{\mathbf{k}}) \tilde{R}_{p'l'}(k) Y_{l'm'}(\hat{\mathbf{k}}), \\
 &= \int dk^3 \left[4\pi \sum_{L=0}^{\infty} \sum_{M=-L}^L (-i)^L j_L(kr) Y_{LM}(\hat{\mathbf{k}}) Y_{LM}^*(\hat{\mathbf{r}}) \right] \tilde{R}_{pl}^*(k) Y_{lm}^*(\hat{\mathbf{k}}) \tilde{R}_{p'l'}(k) Y_{l'm'}(\hat{\mathbf{k}}), \\
 &= 4\pi \sum_{L=0}^{\infty} \sum_{M=-L}^L (-i)^L Y_{LM}^*(\hat{\boldsymbol{\tau}}) C_{l(-m),l'm',LM} \int dk k^2 j_L(k|\boldsymbol{\tau}|) \tilde{R}_{pl}^*(k) \tilde{R}_{p'l'}(k),
 \end{aligned}$$

Forces

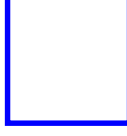
$$\begin{aligned} \mathbf{F}_i &= -\frac{\partial E_{\text{tot}}}{\partial \mathbf{R}_i} \\ &= -\frac{\partial E_{\text{kin}}}{\partial \mathbf{R}_i} - \frac{\partial E_{\text{na}}}{\partial \mathbf{R}_i} - \frac{\partial E_{\text{scc}}}{\partial \mathbf{R}_i} - \frac{\partial E_{\delta\text{ee}}}{\partial \mathbf{R}_i} - \frac{\partial E_{\text{xc}}}{\partial \mathbf{R}_i} - \frac{\partial E_{\text{cc}}}{\partial \mathbf{R}_i} \end{aligned}$$

$$\begin{aligned} \frac{\partial E_{\delta\text{ee}}}{\partial \mathbf{R}_k} &= \sum_{\mathbf{p}} \frac{\partial n(\mathbf{r}_{\mathbf{p}})}{\partial \mathbf{R}_k} \frac{\partial E_{\delta\text{ee}}}{\partial n(\mathbf{r}_{\mathbf{p}})} + \sum_{\mathbf{p}} \frac{\partial n^{\text{a}}(\mathbf{r}_{\mathbf{p}})}{\partial \mathbf{R}_k} \frac{\partial E_{\delta\text{ee}}}{\partial n^{\text{a}}(\mathbf{r}_{\mathbf{p}})}, \\ \frac{\partial E_{\delta\text{ee}}}{\partial n(\mathbf{r}_{\mathbf{p}})} &= \frac{1}{2} \Delta V \{ \delta V_{\text{H}}(\mathbf{r}_{\mathbf{p}}) + \sum_{\mathbf{q}} \delta n(\mathbf{r}_{\mathbf{q}}) \frac{\partial \delta V_{\text{H}}(\mathbf{r}_{\mathbf{q}})}{\partial n(\mathbf{r}_{\mathbf{p}})} \}, \\ &= \frac{1}{2} \Delta V \{ \delta V_{\text{H}}(\mathbf{r}_{\mathbf{p}}) + \frac{4\pi}{N_{\text{rsg}}} \sum_{\mathbf{q}} \frac{1}{|\mathbf{G}|^2} \sum_{\mathbf{q}} \delta n(\mathbf{r}_{\mathbf{q}}) e^{i\mathbf{G} \cdot (\mathbf{r}_{\mathbf{q}} - \mathbf{r}_{\mathbf{p}})} \}, \\ &= \Delta V \delta V_{\text{H}}(\mathbf{r}_{\mathbf{p}}). \end{aligned}$$

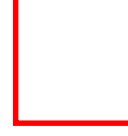
$$\begin{aligned} \frac{\partial E_{\delta\text{ee}}}{\partial n^{\text{a}}(\mathbf{r}_{\mathbf{p}})} &= -\frac{1}{2} \Delta V \{ \delta V_{\text{H}}(\mathbf{r}_{\mathbf{p}}) - \sum_{\mathbf{q}} \delta n(\mathbf{r}_{\mathbf{q}}) \frac{\partial \delta V_{\text{H}}(\mathbf{r}_{\mathbf{q}})}{\partial n^{\text{a}}(\mathbf{r}_{\mathbf{p}})} \}, \\ &= -\frac{1}{2} \Delta V \{ \delta V_{\text{H}}(\mathbf{r}_{\mathbf{p}}) + \frac{4\pi}{N_{\text{rsg}}} \sum_{\mathbf{q}} \frac{1}{|\mathbf{G}|^2} \sum_{\mathbf{q}} \delta n(\mathbf{r}_{\mathbf{q}}) e^{i\mathbf{G} \cdot (\mathbf{r}_{\mathbf{q}} - \mathbf{r}_{\mathbf{p}})} \}, \\ &= -\Delta V \delta V_{\text{H}}(\mathbf{r}_{\mathbf{p}}). \end{aligned}$$

$$\begin{aligned} \frac{\partial n(\mathbf{r}_{\mathbf{p}})}{\partial \mathbf{R}_k} &= \sum_{i\alpha, j\beta} \frac{\partial C_{i\alpha, \nu}^*}{\nu} \frac{\partial C_{j\beta, \nu}}{\partial \mathbf{R}_k} \chi_{i\alpha}(\mathbf{r}) \chi_{j\beta}(\mathbf{r}) + C_{i\alpha, \nu}^* \frac{\partial C_{j\beta, \nu}}{\partial \mathbf{R}_k} \chi_{i\alpha}(\mathbf{r}_{\mathbf{p}}) \chi_{j\beta}(\mathbf{r}_{\mathbf{p}}) \} \\ &\quad + 2 \sum_{\alpha, j\beta} \rho_{k\alpha, j\beta} \frac{\partial \chi_{k\alpha}(\mathbf{r}_{\mathbf{p}})}{\partial \mathbf{R}_k} \chi_{j\beta}(\mathbf{r}_{\mathbf{p}}). \end{aligned}$$

$$\begin{aligned} \frac{\partial E_{\text{xc}}}{\partial \mathbf{R}_k} &= \sum_{\mathbf{p}} \frac{\partial n(\mathbf{r}_{\mathbf{p}})}{\partial \mathbf{R}_k} \frac{\partial E_{\text{xc}}}{\partial n(\mathbf{r}_{\mathbf{p}})}, \\ &= \Delta V \sum_{\mathbf{p}} \frac{\partial n(\mathbf{r}_{\mathbf{p}})}{\partial \mathbf{R}_k} v_{\text{xc}}(n(\mathbf{r}_{\mathbf{p}})). \end{aligned}$$



Easy calc.



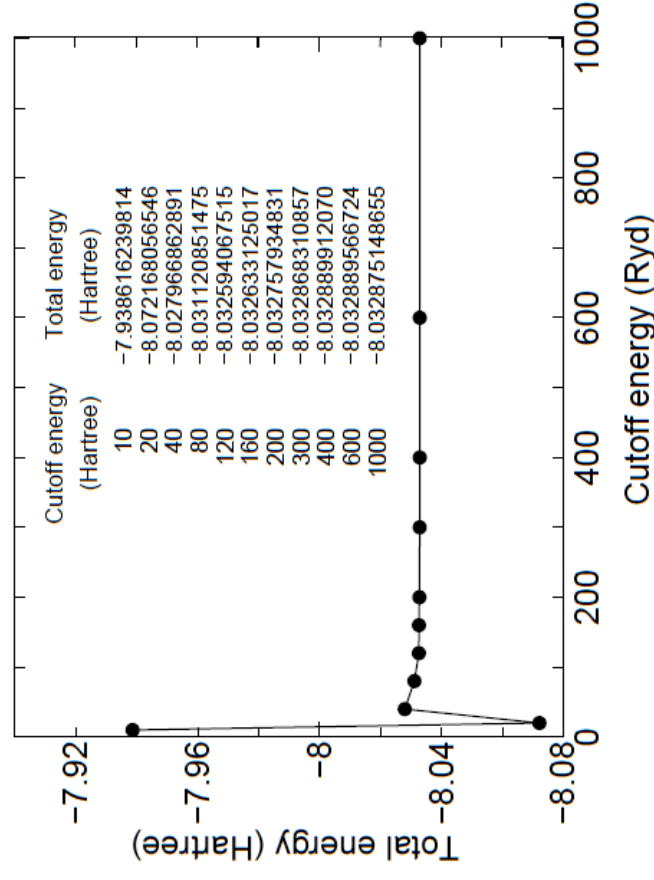
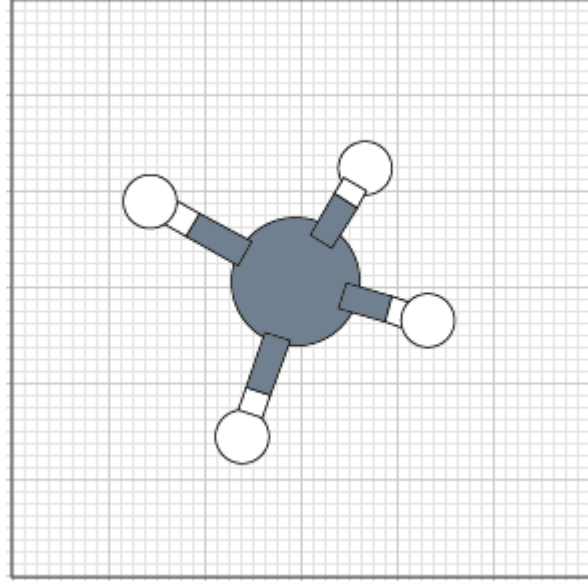
See the left

Forces are always analytic at any grid fineness and at zero temperature, even if numerical basis functions and numerical grids.

Points of concern for reliable & efficient calculations

- ✓ Choice of basis functions
- ✓ **Numerical grid**
- ✓ Quality of pseudopotentials
- ✓ Charge mixing

The proper choice of the cutoff energy depends on system. **150-250 Ryd** is a reasonable choice in most cases.



Points of concern for reliable & efficient calculations

- ✓ Choice of basis functions
- ✓ Numerical grid
- ✓ **Quality of pseudopotentials**

Even though we get convergent results with respect to basis functions and numerical grid, if our results differ from the other calculated results, then the origin of the discrepancy can be attributed to pseudopotentials we used.

Then, we have to return the optimization of pseudopotentials.

Relativistic norm-conserving pseudopotential

Radial Dirac eq. for the majority component

$$\left[\frac{1}{2M(r)} \left(\frac{d^2}{dr^2} + \frac{a^2}{2M(r)} \frac{dV}{dr} + \frac{a^2}{2M(r)} \frac{dV}{dr} - \frac{\kappa(\kappa+1)}{r^2} \right) + \varepsilon_{nlj} - V \right] G_{nlj} = 0$$

$$M(r) = 1 + \frac{a^2(\varepsilon_{nlj} - V)}{2}$$

$\kappa = l$ and $\kappa = -(l+1)$ for $j = l - \frac{1}{2}$ and $j = l + \frac{1}{2}$

For each quantum number j , the Dirac eq. is solved numerically, and its norm-conserving pseudopotential is constructed by the **TM scheme**.

The unified pseudopotential is given by

$$V_{\text{ps}} = \sum_{lm} \left[|\Phi_J^M\rangle V_{\text{ps}}^{l+\frac{1}{2}} \langle \Phi_J^M| + |\Phi_{J'}^{M'}\rangle V_{\text{ps}}^{l-\frac{1}{2}} \langle \Phi_{J'}^{M'}| \right]$$

with the analytic solution for spherical coordinate:

where for $J = l + \frac{1}{2}$ and $M = m + \frac{1}{2}$

$$|\Phi_J^M\rangle = \left(\frac{l+m+1}{2l+1} \right)^{\frac{1}{2}} |Y_l^m\rangle |\alpha\rangle + \left(\frac{l-m}{2l+1} \right)^{\frac{1}{2}} |Y_l^{m+1}\rangle |\beta\rangle,$$

and for $J' = l - \frac{1}{2}$ and $M' = m - \frac{1}{2}$

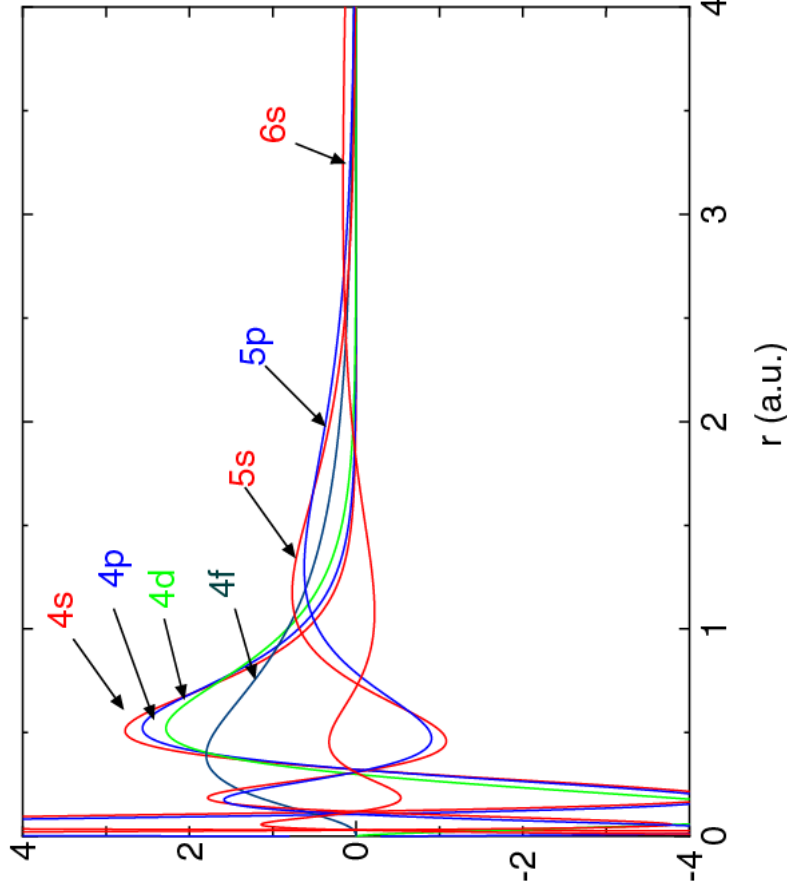
$$|\Phi_{J'}^{M'}\rangle = \left(\frac{l-m+1}{2l+1} \right)^{\frac{1}{2}} |Y_l^{m-1}\rangle |\alpha\rangle - \left(\frac{l+m}{2l+1} \right)^{\frac{1}{2}} |Y_l^m\rangle |\beta\rangle.$$

Relativistic norm-conserving pseudopotential

- All the relativistic effects including the SO coupling are taken into account in the non-collinear calculations.
- In the collinear calculations, the j -dependency is averaged by considering the degeneracy of j , leading to a scalar relativistic pseudopotential.
- The norm-conservation guarantees the correct scattering property around the chosen reference energy for each angular momentum channel.
- The obtained wave function is a pseudo-wave function.
- The non-linearity of exchange-correlation functionals is partially taken into account through the partial core correction.

Difficult case for the TM pseudopotentials (PP)

All electron wave functions of Pr



Eigenvalues (Hartree)

n= 4	l= 0	-10.5170412883091
n= 4	l= 1	-7.9076209877241
n= 4	l= 2	-4.0759804960218
n= 4	l= 3	-0.0525968308191
n= 5	l= 0	-1.4327844478065
n= 5	l= 1	-0.8007101193618
n= 6	l= 0	-0.1346442737184

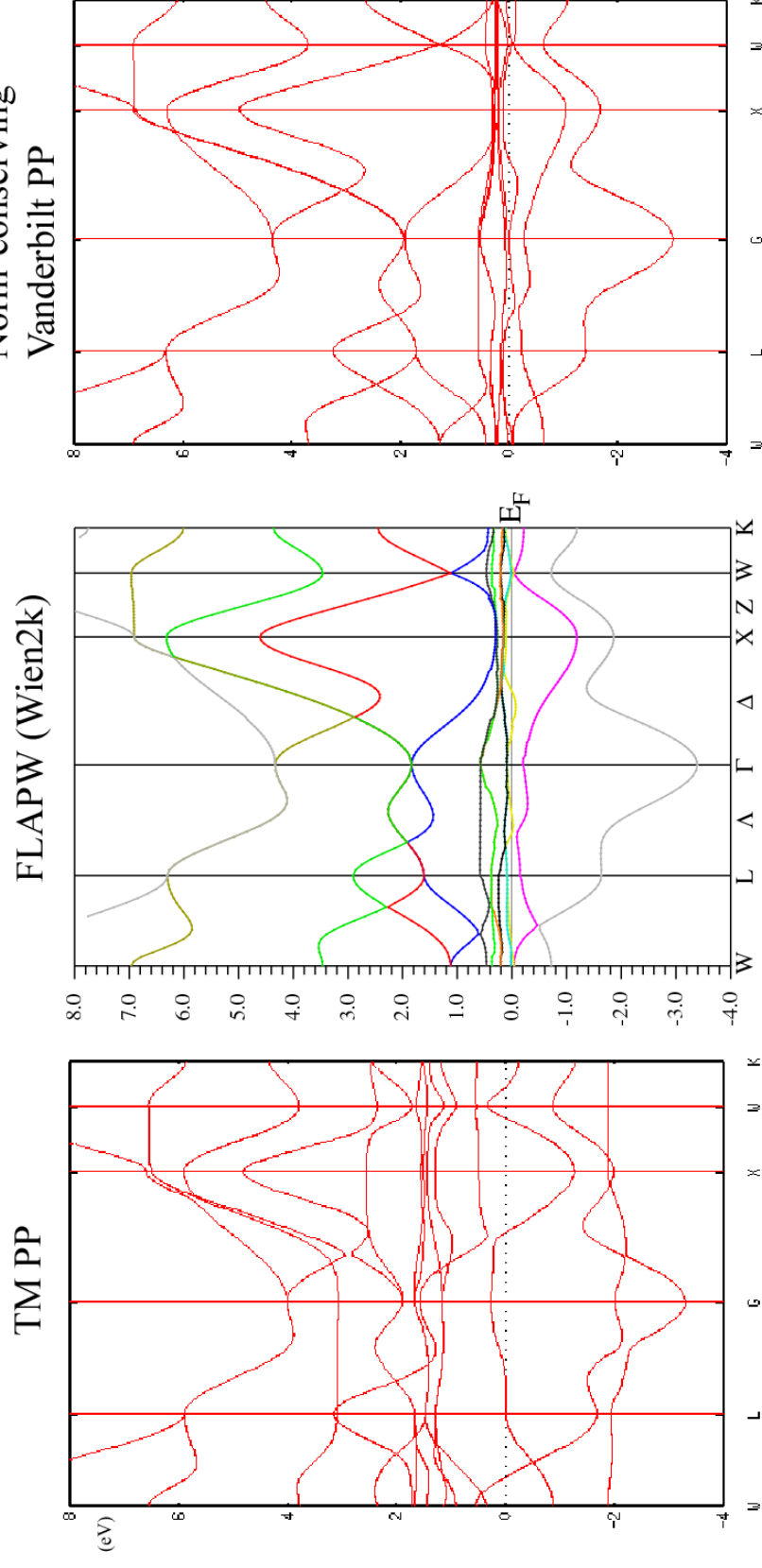
Although the eigenvalue of 4f is close to zero, the peak of the wave function is located in the inner region. This produces a very strong non-linear correlation among 4s, 4p, 4d, 4f, 5s, 5p, and 6s in the exchange-correlation .

Thus, at least it would be better to include 4f, 5s, 5p, and 6s as valence states. However, if the pseudopotential for the s-state is generated for 5s, then the description of the 6s state becomes very poor.

Norm-conserving Vanderbilt PP

We have been developing a norm-conserving Vanderbilt PP which can employ multiple reference energies for each L-channel. (Morrison et al., PRB 47, 6728 (1993))

Comparison in fcc Pr band structure



The norm-conserving Vanderbilt PP looks very promising.

Optimization of pseudopotential

- ✓ The number of valence electrons
- ✓ The number of reference energies
- ✓ Choice of cutoff radii
- ✓ Choice of local part
- ✓ Partial core correction (PCC) charge

Ongoing developments

- $O(N^2)$ method
- Hybrid functionals
- Effective screening medium (ESM) method
- Several methods using Wannier functions
- Improvement of pseudopotentials
- Improvement of basis functions

Summary

OpenMX is a state-of-the-art software package based on the local PAO basis functions and norm-conserving pseudopotentials.

The method can provide reasonable computational accuracy and efficiency in a balanced way for a wide variety of systems including solid state and molecular systems **with careful consideration for the basis functions and pseudopotentials**. The following items should be taken into account by users.

- ✓ Choice of basis functions
- ✓ Numerical grid
- ✓ Quality of pseudopotentials
- ✓ Charge mixing

To improve the reliability and efficiency, and to add more functionalities, the code is still under development.